

# Aryl hydrocarbon receptor activation restores filaggrin expression via OVOL1 in atopic dermatitis

Gaku Tsuji<sup>\*1,2</sup>, Akiko Hashimoto-Hachiya<sup>2</sup>, Mari Kiyomatsu-Oda<sup>2</sup>, Masaki Takemura<sup>2</sup>, Fumitaka Ohno<sup>2</sup>, Takamichi Ito<sup>2</sup>, Saori Morino-Koga<sup>1</sup>, Chikage Mitoma<sup>1,2</sup>, Takeshi Nakahara<sup>2,3</sup>, Hiroshi Uchi<sup>2</sup> and Masataka Furue<sup>1,2,3</sup>

Filaggrin (*FLG*) mutation is a well-confirmed genetic aberration in atopic dermatitis (AD). Genome-wide association studies on AD have revealed other susceptibility genes, for example, Ovo-like 1 (*OVOL1*). Nonetheless, the relation between *FLG* and *OVOL1* is unclear. Because aryl hydrocarbon receptor (AHR; a ligand-activated transcription factor), plays a role in *FLG* expression in keratinocytes, we hypothesized that AHR regulates *FLG* expression via *OVOL1*. To demonstrate this mechanism, we analyzed *FLG* expression in *OVOL1*-overexpressing or *OVOL1*-knockdown normal human epidermal keratinocytes (NHEKs). Furthermore, we tested whether AHR activation by 6-formylindolo(3,2-b)carbazole (FICZ), an endogenous AHR ligand, or Glyteer, clinically used soybean tar, upregulates *FLG* and *OVOL1* expression in NHEKs. We found that (1) *OVOL1* regulates *FLG* expression; (2) AHR activation upregulates *OVOL1*; and (3) AHR activation upregulates *FLG* via *OVOL1*. Moreover, nuclear translocation of *OVOL1* was less pronounced in AD skin compared with normal skin. IL-4-treated NHEKs, an *in vitro* AD skin model, also showed inhibition of the *OVOL1* nuclear translocation, which was restored by FICZ and Glyteer. Thus, targeting the AHR–*OVOL1*–*FLG* axis may provide new therapeutics for AD.

*Cell Death and Disease* (2017) 8, e2931; doi:10.1038/cddis.2017.322; published online 13 July 2017

Mammalian epidermis comprises stratified squamous keratinocytes that protect the body from injuries by external (e.g., environmental) factors. Cornified envelope maturation is accomplished via sequential and coordinated cross-linking of ceramides and various skin barrier proteins, such as filaggrin (*FLG*), by transglutaminases 1 and 3.<sup>1</sup> Recent studies revealed that disruption of the barrier function is crucial for the development of not only atopic dermatitis (AD) but also other allergic disorders, including asthma, allergic rhinitis, and food allergies.<sup>2,3</sup> Furthermore, a loss-of-function mutation of *FLG* is a well-confirmed genetic aberration associated with AD among different ethnic groups.<sup>4,5</sup> Therefore, clarifying the mechanism regulating *FLG* expression and establishing a strategy for increasing *FLG* expression may be beneficial for the treatment of AD.

Our recent studies have shown that activation of aryl hydrocarbon receptor (AHR), a ligand-activated transcription factor, is a key determinant of *FLG* expression in normal human epidermal keratinocytes (NHEKs).<sup>6,7</sup> Activated AHR relocates from the cytoplasm to nucleus, and this action induces transcription of the target genes, such as *CYP1A1*, in NHEKs. Nonetheless, the precise mechanism by which AHR regulates *FLG* expression remains unclear.

A series of genome-wide association studies conducted in Europe, China, and Japan have revealed other susceptibility genes, such as *OVOL1*, which is related to epidermal differentiation.<sup>8–13</sup> *OVOL1* is a ubiquitously conserved gene encoding a C2H2 zinc finger transcription factor in mammals. Functional studies in *Caenorhabditis elegans*, *Drosophila*

*melanogaster*, and *Mus musculus* have suggested that this gene plays a pivotal role in the development of epithelial tissues arising from germ cells.<sup>14–16</sup> Our studies and those conducted by other researchers have shown that *OVOL1* is expressed in multiple somatic epithelial tissues, including human skin.<sup>14,17,18</sup> Recent studies indicate that *OVOL1* activation redirects cell proliferation to cell differentiation,<sup>16,19</sup> pointing to the possibility that *OVOL1* controls the expression of skin barrier proteins, including *FLG*, during keratinocyte differentiation. Our recent study indicates that AHR activation by ketoconazole, a potent AHR ligand,<sup>20</sup> upregulates *OVOL1* in NHEKs.<sup>18</sup> Therefore, we hypothesized that AHR upregulates *FLG* via *OVOL1* and that *OVOL1* impairment is involved in *FLG* downregulation, which may possibly contribute to the development of AD.

To test this hypothesis, we analyzed *FLG* expression in *OVOL1*-overexpressing or *OVOL1*-knockdown NHEKs using the methods of electroporation and small interfering RNA (siRNA) transfection. Furthermore, to determine whether AHR activation upregulates or downregulates *OVOL1* and *FLG*, we used 6-formylindolo(3,2-b)carbazole (FICZ), an endogenous AHR ligand, and Glyteer, a soybean tar clinically used in Japan.

It has been already shown that AHR activation induced by coal tar increases *FLG* expression contributing to the therapeutic effect of coal tar on the development of AD;<sup>21</sup> however, whether *OVOL1* is involved in the upregulation of *FLG* induced by AHR activation has not been examined.

<sup>1</sup>Research and Clinical Center for Yusho and Dioxin, Kyushu University, Maidashi 3-1-1, Higashiku, Fukuoka 812-8582, Japan; <sup>2</sup>Department of Dermatology, Graduate School of Medical Sciences, Kyushu University, Maidashi 3-1-1, Higashiku, Fukuoka 812-8582, Japan and <sup>3</sup>Division of Skin Surface Sensing, Graduate School of Medical Sciences, Kyushu University, Maidashi 3-1-1, Higashiku, Fukuoka 812-8582, Japan

\*Corresponding author: G Tsuji, Research and Clinical Center for Yusho and Dioxin, Kyushu University, Maidashi 3-1-1, Higashiku, Fukuoka 812-8582, Japan. Tel: +81 92 642 5585; Fax: +81 92-642-5600; E-mail: gaku@dermatol.med.kyushu-u.ac.jp

Received 12.2.17; revised 01.6.17; accepted 05.6.17; Edited by E Candi

Herein, we demonstrate that *OVOL1* is an integral part for the AHR-mediated FLG expression in human keratinocytes.

## Results

To examine the function of *OVOL1* in *FLG* expression in NHEKs, we established either *OVOL1*-overexpressing (*OVOL1* OE) NHEKs by electroporating the plasmid containing an open reading frame of human *OVOL1* into NHEKs or knocked *OVOL1* down via transfection of *OVOL1* siRNA. *FLG* expression was increased in *OVOL1* OE NHEKs (Figure 1a). Conversely, *FLG* expression was significantly decreased in NHEKs transfected with *OVOL1* siRNA (Figure 1b), indicating that *OVOL1* is intimately involved in *FLG* expression in NHEKs. Compared with mock-transfected NHEKs (Figure 1c), the protein levels of FLG in *OVOL1* OE NHEKs (Figure 1d) were increased according to immunofluorescence analysis with an anti-FLG antibody. The protein levels of *OVOL1* either in *OVOL1* OE NHEKs or *OVOL1*-knockdown NHEKs were evaluated by western blotting with an anti-*OVOL1* antibody (Supplementary Figures S1A and B); this experiment confirmed that both types of transfection were successful. Next, to test whether *OVOL1* regulates other genes of the epidermal differentiation complex including loricrin (*LOR*), involucrin (*IVL*), and transglutaminase 1 (*TGM1*) (representative terminal differentiation markers of keratinocytes), we analyzed *LOR*, *IVL*, and *TGM1* expression in *OVOL1* OE NHEKs and *OVOL1*-knockdown NHEKs. In agreement with another report,<sup>16</sup> *LOR*, but not *IVL* or *TGM1* expression was increased in *OVOL1* OE NHEKs (Supplementary Figure S1C) and decreased in *OVOL1*-knockdown NHEKs (Supplementary Figure S1D). Therefore, *OVOL1* specifically regulates *FLG* and *LOR* expression, contributing to the terminal differentiation of human keratinocytes.

Given that our previous studies revealed that AHR activation induces *FLG* expression in NHEKs,<sup>6</sup> we determined whether AHR regulates the *OVOL1* expression in NHEKs. *OVOL1* expression was decreased in AHR-knockdown NHEKs transfected with AHR siRNA as compared with the cells transfected with control siRNA (Supplementary Figure S2A). The protein levels of AHR were evaluated by western blotting with an anti-AHR antibody (Supplementary Figure S2B); this assay confirmed that the knockdown of AHR by the transfection of siRNA against AHR was successful.

We next examined the effects of an AHR ligand on *OVOL1* and *FLG* expression. AHR activation by FICZ or Glyteer significantly upregulated *OVOL1* in a dose- and time-dependent manner (Figures 2a–d). The activation of AHR by FICZ or Glyteer also significantly increased *FLG* expression in a dose- and time-dependent manner (Figures 2e–h). Consistent with these results, AHR activation by FICZ or Glyteer increased *OVOL1* and *FLG* expression in a dose- and time-dependent manner in a western blot analysis (Figures 2i and j).

To test whether FICZ and Glyteer upregulate *OVOL1* and *FLG* via AHR, we analyzed FICZ- or Glyteer-treated NHEKs transfected with control siRNA or anti-AHR siRNA. The upregulation of *OVOL1* by FICZ (Figure 3a) and Glyteer (Figure 3b) was abrogated in AHR-knockdown NHEKs. Moreover, the upregulation of *FLG* by FICZ (Figure 3c) and

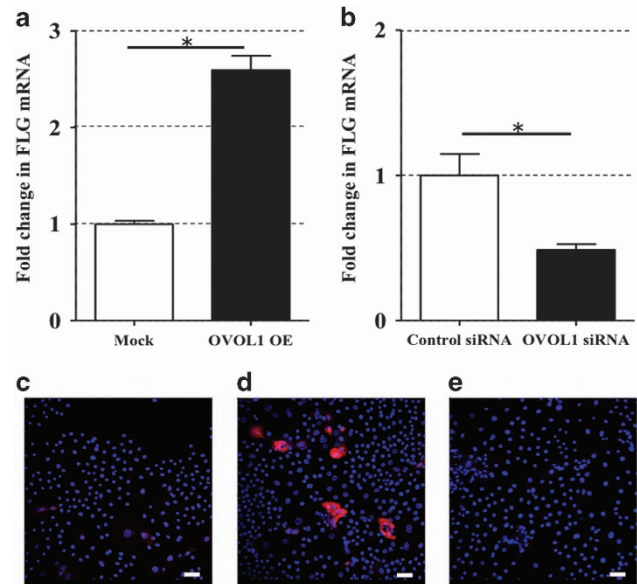


**Figure 1** *OVOL1* regulated *FLG* expression in NHEKs. (a and b) Data are expressed as mean  $\pm$  S.E.M.;  $n=3$  for each group;  $*P<0.05$ . (a) *OVOL1* was overexpressed in NHEKs (*OVOL1* OE cells) by electroporation of the plasmid containing an open reading frame of human *OVOL1*. *FLG* expression in the *OVOL1* OE cells was analyzed by qRT-PCR. (b) *OVOL1* was knocked down by transfection of *OVOL1* siRNA into NHEKs (*OVOL1* siRNA cells). *FLG* expression in *OVOL1* siRNA NHEKs was analyzed by qRT-PCR. Mock-transfected NHEKs (c) and *OVOL1* OE NHEKs (d) were stained with an anti-*FLG* antibody (primary antibody) and an Alexa Fluor 546-conjugated anti-mouse IgG antibody (secondary). The nuclei were counterstained with DAPI (blue). Confocal laser scanning images revealed increased *FLG* expression (red) in *OVOL1* OE NHEKs compared with mock-transfected NHEKs. (e) Isotype negative control. The scale bar is 25  $\mu$ m. The data are representative of experiments repeated three times with similar results

Glyteer (Figure 3d) was abrogated in AHR-knockdown NHEKs and *OVOL1*-knockdown NHEKs. In the immunofluorescence analysis using the anti-*FLG* antibody, the upregulation of *FLG* induced by FICZ was abrogated in AHR-knockdown NHEKs and *OVOL1*-knockdown NHEKs (Figures 3e–j). Glyteer also showed the same pattern (Supplementary Figures S3A–C). These results indicate that FICZ and Glyteer upregulate *FLG* via the AHR – *OVOL1* axis in NHEKs. Because the monolayer-cultured NHEKs system was difficult to use for evaluation of protein expression of *FLG*, including profilaggrin expression,<sup>7</sup> we utilized three-dimensionally (3D) cultured NHEKs. In the western blot analysis, FICZ and Glyteer yielded increased *OVOL1* and *FLG* protein expression, which was normalized by CH-223191, a specific antagonist of AHR (Figure 3l). This finding also confirmed that AHR activation increases *OVOL1* and *FLG* protein levels.

To identify the role of *OVOL1* and *FLG* in the AD pathogenesis, we evaluated *OVOL1* and *FLG* expression in clinical samples of either normal skin or AD skin by immunohistochemical (IHC) staining. Compared with normal skin (Figures 4a and b), *FLG* expression was lower in AD skin (Figures 4d and e); this finding is consistent with another study.<sup>22</sup>

The expression of *OVOL1* was observed mainly in the nucleus of keratinocytes in normal skin (Figure 4c); however,

OVOL1 was not expressed in the FLG-positive cells in normal skin. As shown in Figures 2i and j, the FICZ- and Glyteer-induced upregulation of OVOL1 expression peaked at 24 h and gradually diminished until 48 h. In contrast, the FICZ- and

Glyteer-induced FLG expression was observed to increase at 72 h. Therefore, the gap between the expression levels of OVOL1 and FLG in keratinocytes in the IHC staining experiment presumably resulted from the lag of the expression of OVOL1 and FLG in human keratinocytes.

The nuclear OVOL1 expression was lower in AD skin (Figures 4f and g) compared with normal skin, suggesting that nuclear translocation of OVOL1 is likely to be inhibited in AD skin. Because OVOL1 performs a transcription-regulatory function in the nucleus,<sup>18</sup> these results suggest that the transcription-regulatory activity of OVOL1 may be impaired in AD skin, subsequently leading to the reduced FLG expression in AD skin.

To identify the mechanism by which the OVOL1 nuclear translocation is inhibited in AD skin, we analyzed OVOL1 expression in NHEKs treated with IL-4, a powerful suppressor of FLG expression; treatment with IL-4 can serve as an *in vitro* AD model.<sup>7,21</sup> Our previous study has shown that steady-state OVOL1 expression is primarily present in the cytoplasm of NHEKs.<sup>18</sup> Ketoconazole, a potent AHR ligand, induces nuclear translocation of OVOL1 in NHEKs.<sup>18</sup> Therefore, we used immunofluorescence analysis to test whether IL-4 affects the cytoplasm-to-nucleus translocation of OVOL1 in NHEKs. OVOL1 was stained with an anti-OVOL1 antibody (primary antibody) and an Alexa Fluor 488-conjugated anti-rabbit IgG antibody (secondary), which emits bright green fluorescence. 4',6-Diamidino-2-phenylindole (DAPI), which emits blue fluorescence, was used for nuclear counterstaining. We determined whether the two-color fluorescent signals (green and blue) coincided in the nucleus to detect the OVOL1 nuclear translocation. In baseline NHEKs, OVOL1 expression was noted mainly in the cytoplasm (Figure 4h). Just as ketoconazole, the activation of AHR by FICZ clearly induced the nuclear translocation of OVOL1 (Figure 4i). In contrast, IL-4 did not induce OVOL1 nuclear translocation, and OVOL1 was retained in the cytoplasm (Figure 4j). IL-4-mediated blockade of the OVOL1 nuclear translocation was overcome by treatment with FICZ (Figure 4k). Similar results were obtained with Glyteer (Supplementary Figures S4A and B). These results were confirmed by western blot analysis. NHEKs were treated with FICZ (100 nM) or Glyteer (0.001%) in the absence or presence of IL-4 (10 ng/ml) for 18 h. Cell nuclear protein was extracted using a biochemical subcellular fractionation technique. The OVOL1 levels in the nuclear protein fraction of NHEKs were evaluated by western blotting. Histone deacetylase 1 (HDAC1) served as an internal loading control. The activation of AHR by FICZ increased the nuclear OVOL1

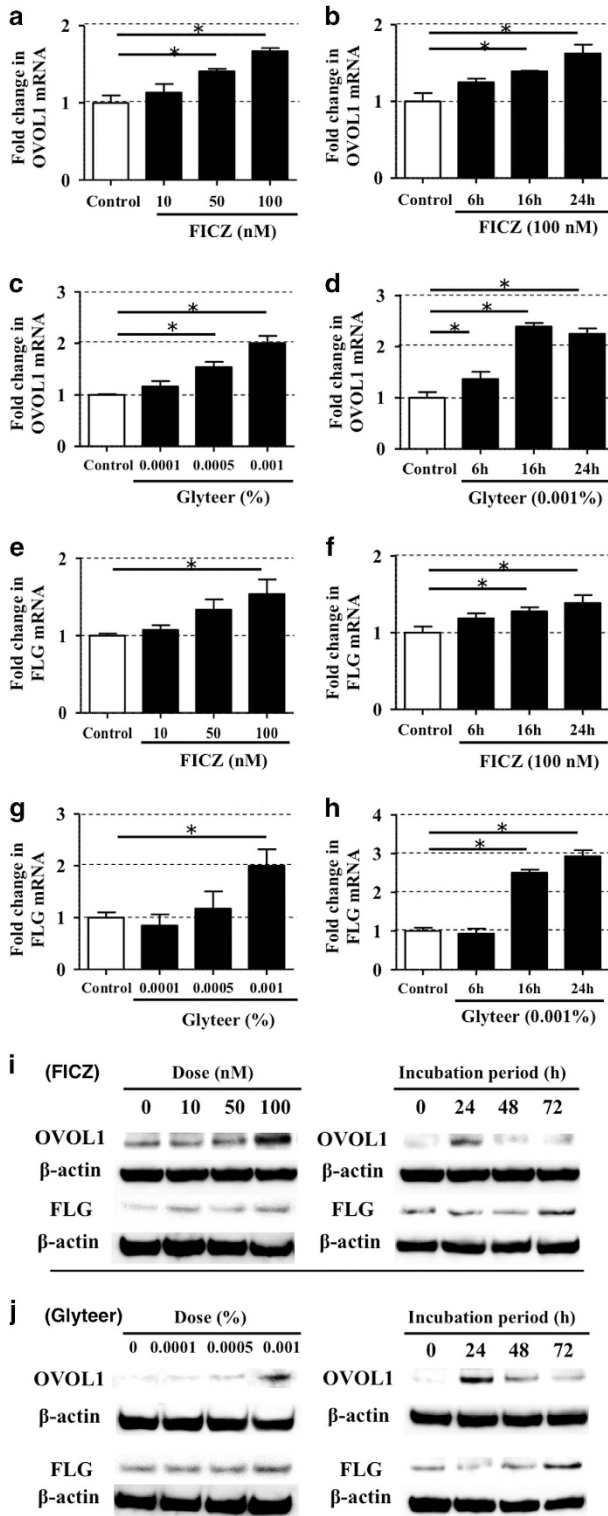


**Figure 2** AHR activation induced by FICZ and Glyteer increased the expression of OVOL1 and FLG in a dose- and time-dependent manner in NHEKs. Data are expressed as mean  $\pm$  S.E.M.;  $n = 3$  for each group;  $*P < 0.05$ . (a, c, e, and g) NHEKs were treated with FICZ or Glyteer at the indicated dose for 24 h. (b, d, f, and h) NHEKs were treated with FICZ (100 nM) or Glyteer (0.001%) for the indicated period. (a–h) Expression of *FLG* and *OVOL1* was analyzed by qRT-PCR. (i and j) NHEKs were treated with FICZ or Glyteer at the indicated dose for 24 h or for the indicated period. Total cell lysates were prepared and subjected to western blot analysis with an anti-FLG antibody and anti-OVOL1 antibody. The data are representative of experiments repeated three times with similar results

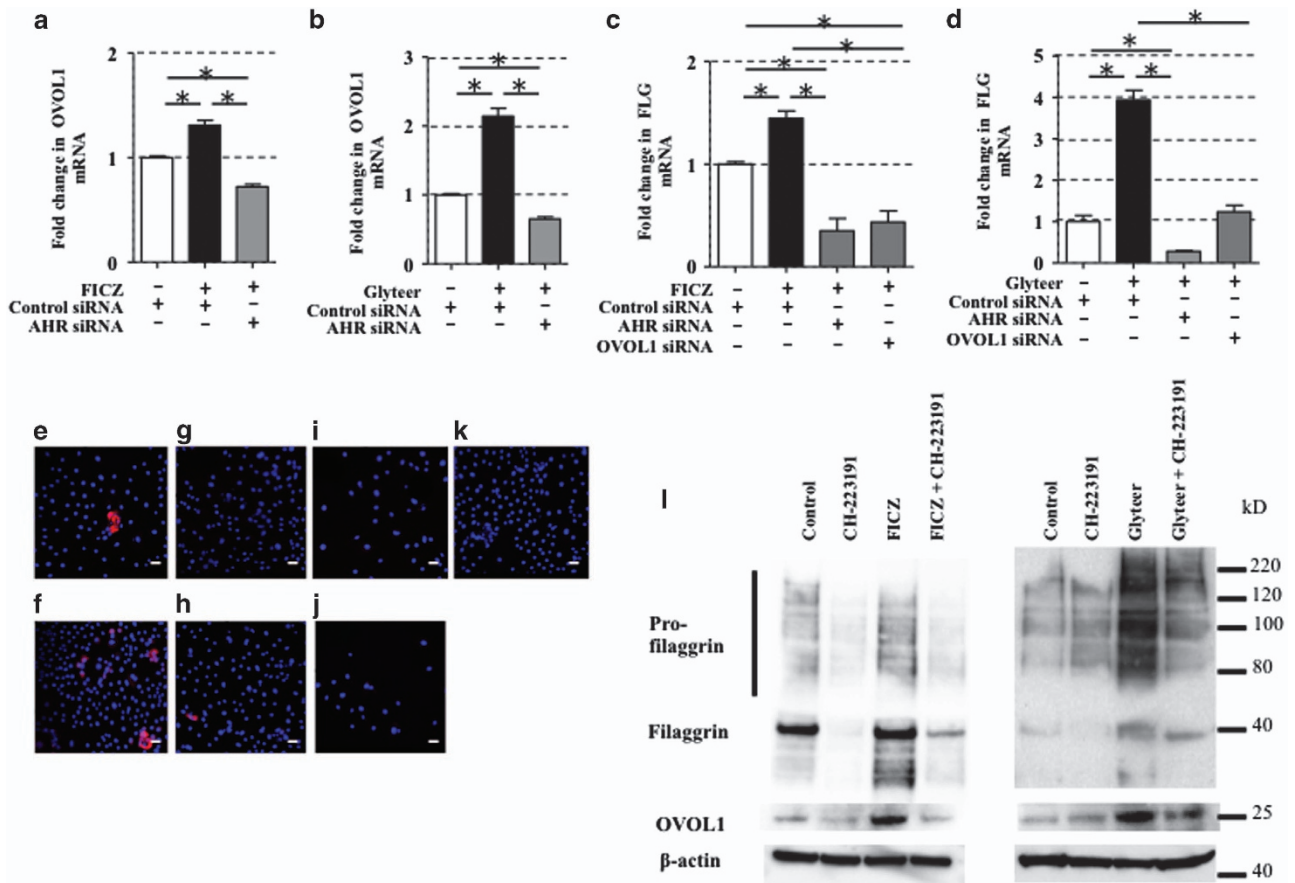


**Figure 3** AHR regulated FLG expression via OVOL1 in NHEKs. (a–d) Data are expressed as mean  $\pm$  S.E.M.;  $n=3$  for each group;  $*P<0.05$ . NHEKs were transfected with control siRNA or AHR siRNA and then treated with FICZ (100 nM) or Glyteer (0.001%) for 24 h. Expression of *OVOL1* and *FLG* in the NHEKs was analyzed by qRT-PCR. (e–k) NHEKs transfected with control siRNA, AHR siRNA, or OVOL1 siRNA were treated with DMSO or FICZ (100 nM) for 24 h and then stained with an anti-FLG antibody (primary antibody) and an Alexa Fluor 546-conjugated anti-mouse IgG antibody (secondary). The nuclei were counterstained with DAPI (blue). (e) Control siRNA-transfected NHEKs treated with DMSO, (f) control siRNA-transfected NHEKs treated with FICZ, (g) AHR siRNA-transfected NHEKs treated with DMSO, (h) AHR siRNA-transfected NHEKs treated with FICZ, (i) OVOL1 siRNA-transfected NHEKs treated with DMSO, and (j) OVOL1 siRNA-transfected NHEKs treated with FICZ. (k) Isotype negative control. Confocal laser scanning images revealed increased FLG expression (red) in control siRNA-transfected NHEKs treated with Glyteer (f) as compared with control siRNA-transfected NHEKs treated with DMSO (e); this upregulation was abrogated in AHR siRNA- or OVOL1 siRNA-transfected NHEKs treated with FICZ (h and j). The data are representative of experiments repeated three times with similar results. The scale bar is 25  $\mu$ m. (l) 3D-cultured NHEKs were treated with CH-223191 (10  $\mu$ M), FICZ (1  $\mu$ M), or CH-223191 (10  $\mu$ M) plus FICZ (1  $\mu$ M), or CH-223191 (10  $\mu$ M), Glyteer (0.01%), or CH-223191 (10  $\mu$ M) plus Glyteer (0.01%) for 48 h. Total cell lysates were prepared and subjected to western blot analysis with an anti-FLG antibody and an anti-OVOL1 antibody. The data are representative of experiments repeated three times with similar results

expression; in contrast, IL-4 did not change nuclear expression of OVOL1. The IL-4-mediated blockade of the OVOL1 nuclear translocation was partially reversed by treatment with FICZ (Figure 4m). A similar result was obtained with Glyteer (Supplementary Figure S4C).

In line with these results, FICZ and Glyteer reversed the IL-4-induced FLG downregulation in mRNA levels (Figures 5a and b) and protein levels (Figure 5c). To further elucidate whether OVOL1 is involved in the IL-4-induced *FLG* downregulation, we analyzed OVOL1-knockdown NHEKs treated with FICZ or Glyteer plus IL-4. The ability of FICZ or Glyteer to reverse the IL-4-induced FLG downregulation was abrogated in OVOL1-knockdown NHEKs (Figures 5a–c). We hypothesized that IL-4 inhibits *OVOL1* expression in NHEKs; however, this was not the case. Rather, IL-4 increased the baseline, FICZ-induced, or Glyteer-induced *OVOL1* expression (Supplementary Figure S5).

## Discussion

*Ovol1* has been shown to be a transcriptional factor important for the expression of murine epidermal differentiation complex genes, including *Fgf*, *Ivl*, and *Lor*.<sup>16,23</sup> Furthermore, genetic depletion of *Ovol1* results in downregulation of *Fgf* expression in murine keratinocytes.<sup>23</sup> Therefore, *Ovol1* possibly regulates the expression of *Fgf* in murine keratinocytes transcriptionally; however, the precise mechanism in human keratinocytes has not been fully examined.

In agreement with these findings, our previous study showed that OVOL1 and OVOL2 are preferentially expressed in human keratinocytes, indicating that the OVOL1–OVOL2 axis coordinately controls human keratinocyte differentiation.<sup>18</sup> In the present study, we demonstrated that *OVOL1* is an integral part of the AHR-mediated mechanism of FLG expression in human keratinocytes.

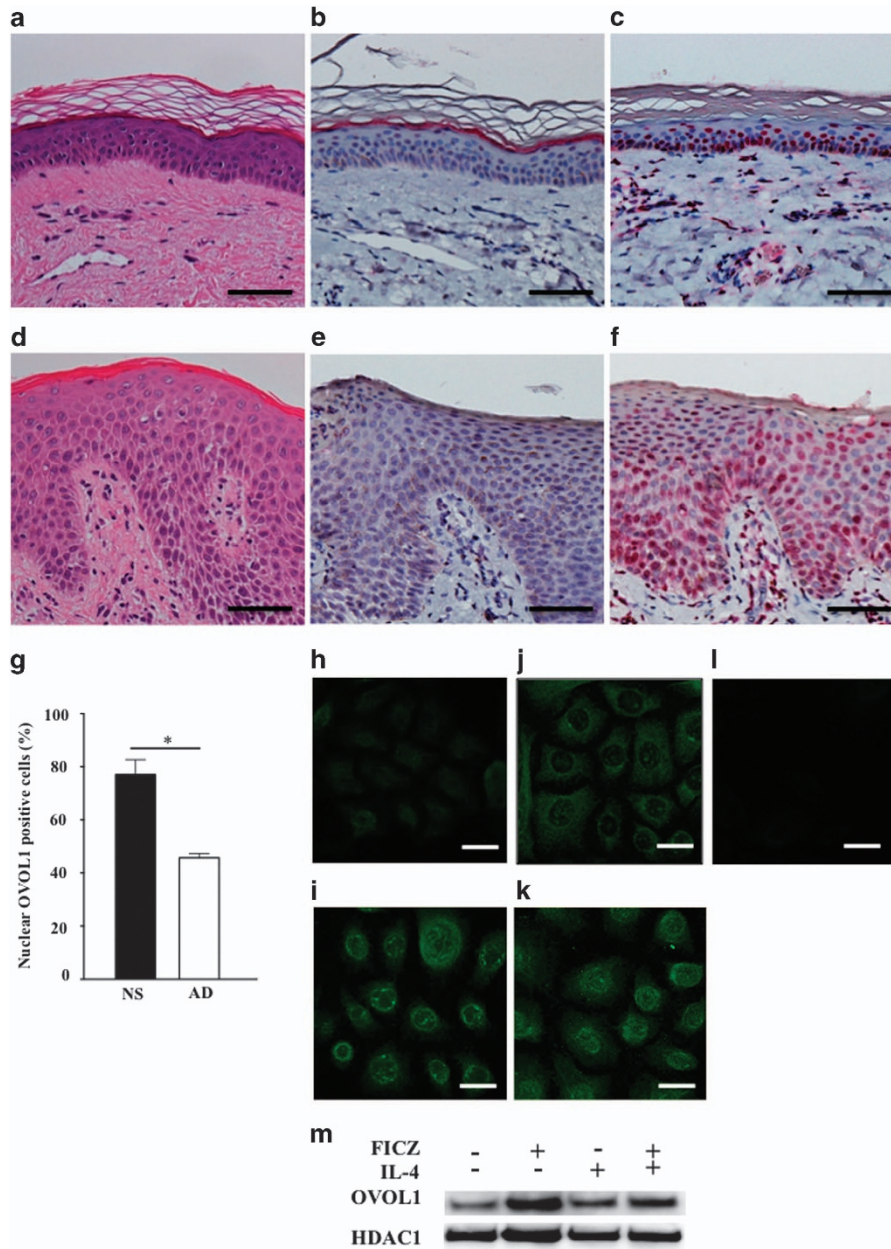


**Figure 4** Nuclear translocation of OVOL1 was likely to be inhibited in AD skin, leading to the reduced FLG expression in AD skin. Normal skin (a) and AD skin (d) were stained with hematoxylin and eosin. The scale bar is 100  $\mu$ m. Expression of FLG and OVOL1 in the epidermis of the same skin lesion was analyzed by IHC staining for FLG (red) or OVOL1 (red). The expression of FLG was observed in normal skin (b) and was low in AD skin (e). The expression of OVOL1 was observed mainly in the nuclei of keratinocytes in normal skin (c); however, nuclear OVOL1 expression was lower in AD skin (f). For semiquantitative analysis of IHC staining, microscopic visual fields of the samples from each group were randomly chosen and examined. In a high-power field (x400 magnification), the nuclear-OVOL1-stained cells of the epidermis were counted, as were all the cells with hematoxylin staining. Nuclear OVOL1 expression was lower in AD skin (AD) compared with normal skin (NS) (g). NHEKs treated with DMSO (h), FICZ (100 nM) (i), IL-4 (10 ng/ml) (j), or FICZ plus IL-4 (k) for 24 h were stained with an anti-OVOL1 antibody (primary antibody) and an Alexa Fluor 488-conjugated anti-rabbit IgG antibody (secondary). The nuclei were counterstained with DAPI (blue). Confocal laser scanning images revealed that OVOL1 expression was noticeable mainly in the cytoplasm in a steady state (h) and that the AHR activation by FICZ induced nuclear translocation of OVOL1 (i). In contrast, IL-4 did not induce nuclear translocation of OVOL1, and the latter was retained in the cytoplasm (j). IL-4-mediated blockade of the nuclear translocation of OVOL1 was overridden by treatment with FICZ (k). (l) Isotype negative control. The scale bar is 25  $\mu$ m. The data are representative of experiments repeated three times with similar results. (m) NHEKs were treated with FICZ (100 nM) in the absence or presence of IL-4 (10 ng/ml) for 18 h. Cellular nuclear protein was extracted using a biochemical subcellular fractionation technique. The OVOL1 levels in the nuclear protein fraction of NHEKs were evaluated by western blotting. The activation of AHR by FICZ increased the nuclear OVOL1 expression; in contrast, IL-4 did not change nuclear expression of OVOL1. The IL-4-mediated blockade of the OVOL1 nuclear translocation was partially reversed by treatment with FICZ. The data are representative of experiments repeated three times with similar results

The finding that *OVOL1* positively regulates *FLG* expression provides an important insight into the known phenomenon of reduced *FLG* expression in AD patients. Recent genome-wide association studies on AD have identified three single-nucleotide polymorphisms (SNPs), rs479844 (*OVOL1*),

rs3126085 (*FLG*), and rs11204971 (*FLG*), that are associated with AD in Japanese and Chinese patients.<sup>8–13</sup> The A allele of rs479844 (*OVOL1*) reportedly reduces AD risk.<sup>24</sup> Furthermore, *FLG* mutation or dysfunction is a crucial factor in AD development.<sup>4,5</sup> Therefore, we can hypothesize that *OVOL1* impairment results in the downregulation of *FLG*, thus potentiating the development of AD.

We and other researchers have demonstrated that tar derived from coal or soybeans clinically used in Japan upregulates *FLG* via AHR activation, contributing to improvement of the barrier function in AD.<sup>7,21</sup> It has been shown in AHR knockdown NHEKs<sup>21</sup> that an AHR-binding site (xenobiotic response element) in the *FLG* promoter region has an important role in the upregulation of *FLG* induced by AHR activation. Nevertheless, we next revealed that the upregulation of *FLG* induced by AHR activation was abrogated in either AHR knockdown or *OVOL1*-knockdown NHEKs.

We found that the *OVOL1* promoter between genomic positions 65786247 and 65787182 (NCBI Reference Sequence: NC\_000011.10) contains three 'GCGTG' (xenobiotic response element) sites. This notion is in agreement with the fact that ketoconazole, an AHR activator, increases *OVOL1* expression in NHEKs, underscoring the possibility that AHR transcriptionally mediates *OVOL1* expression in NHEKs. The present study clearly showed that *OVOL1* levels correlate with *FLG* mRNA and protein levels and that AHR-mediated *FLG* upregulation is abrogated in *OVOL1*-knockdown NHEKs. To further characterize the involvement of *OVOL1* in the pathogenesis of AD, we analyzed *OVOL1* expression in clinical samples of AD skin and in IL-4-treated NHEKs. To the best of our knowledge, here we for the first time showed that nuclear translocation of *OVOL1* is inhibited in AD skin. On the basis of these results, we assumed that the blockade of *OVOL1* nuclear translocation may be responsible for the inhibitory action of IL-4 on *FLG* expression. The activation of AHR by FICZ and Glyteer reversed the IL-4-induced blockade and facilitated the cytoplasm-to-nucleus translocation of *OVOL1*, thereby increasing *FLG* transcription (Figure 6). Given that FICZ, a photoproduct of tryptophan, is generated by ultraviolet irradiation in the skin,<sup>25</sup> it is possible that phototherapy improves the skin condition in AD via the

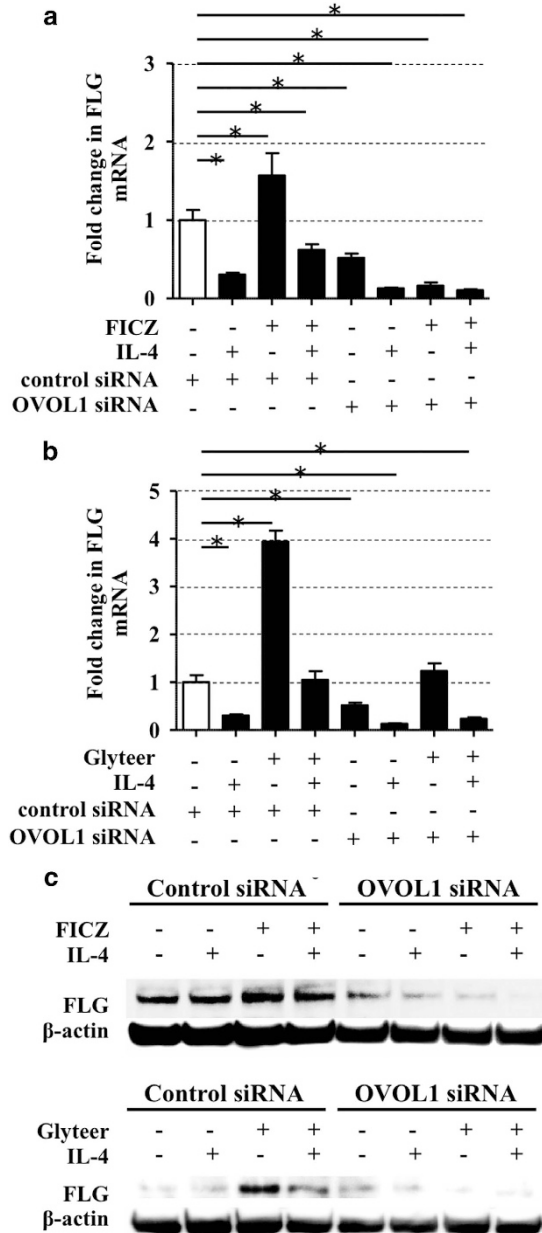


**Figure 5** FICZ and Glyteer reversed the IL-4-induced decrease in *FLG* expression, which was dependent on *OVOL1*. Control siRNA- or *OVOL1* siRNA-transfected NHEKs were treated with FICZ (100 nM) (a) or Glyteer (0.001%) (b) with or without IL-4 (10 ng/ml) for 24 h and then mRNA or total protein of the NHEKs were extracted. Expression of *FLG* in the NHEKs was analyzed by qRT-PCR. Data are expressed as mean  $\pm$  S.E.M.;  $n=3$  for each group;  $*P<0.05$ . (c) Expression of *FLG* was analyzed by western blotting using the anti-*FLG* antibody. The data are representative of experiments repeated three times with similar results. The ability of FICZ or Glyteer to reverse the IL-4-induced downregulation of *FLG* was abrogated in *OVOL1*-knockdown NHEKs

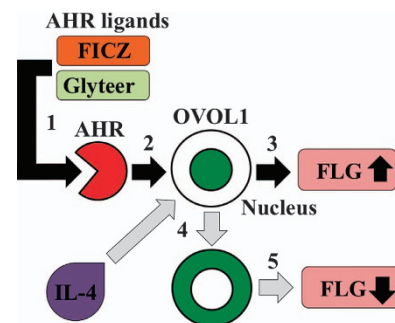


**Figure 6** AHR activation induced by FICZ and Glyteer restores *FLG* expression via *OVOL1* in the skin affected by atopic dermatitis (AD). 1. FICZ and Glyteer bind to AHR thereby leading to AHR activation. 2. Activated AHR induces upregulation and nuclear translocation of *OVOL1*. 3. The *OVOL1* nuclear translocation of *OVOL1* increases *FLG* expression. 4. IL-4 inhibits the nuclear translocation of *OVOL1*. 5. Inhibition of the nuclear translocation of *OVOL1* downregulates *FLG*

AHR–OVOL1–FLG pathway. Nevertheless, the precise mechanism by which IL-4 inhibits the nuclear translocation of OVOL1 remains unclear, and further studies are needed.

Thus, we demonstrated that OVOL1 positively controls FLG expression and that AHR regulates FLG expression via OVOL1 in NHEKs. These results suggest that a potent AHR–OVOL1 activator may have a therapeutic potential in AD via upregulation of *FLG*.

## Materials and Methods

**Reagents and antibodies.** FICZ was purchased from Enzo Life Sciences (Exeter, UK). Glyteer was provided as an original stock solution by Fujinaga Pharm Co. Ltd. (Tokyo, Japan). DMSO and CH-223191 were purchased from Sigma-Aldrich (St. Louis, MO). IL-4 was purchased from R&D Systems (Minneapolis, MN, USA). For western blotting analysis, an anti-AHR rabbit polyclonal IgG antibody (Santa Cruz Biotechnology, Dallas, TX, USA), anti-OVOL1 mouse monoclonal antibody (Abcam, Cambridge, UK), and anti-FLG mouse antibody (Santa Cruz Biotechnology) were used. For immunofluorescent staining and IHC analysis, an anti-OVOL1 rabbit polyclonal antibody (LifeSpan BioSciences, Inc., Seattle, WA, USA) and anti-FLG mouse monoclonal antibody (Abcam) were applied. Normal rabbit IgG was purchased from Santa Cruz Biotechnology.

**Cell culture.** NHEKs obtained from Clonetics-BioWhittaker (San Diego, CA, USA) were grown in culture dishes at 37 °C and 5% CO<sub>2</sub>. NHEKs were cultured in a serum-free keratinocyte growth medium (Lonza, Walkersville, MD, USA) supplemented with bovine pituitary extract, recombinant epidermal growth factor, insulin, hydrocortisone, transferrin, and epinephrine. The culture medium was replaced every 2 days. Near-confluent (70–90%) cells were disaggregated with 0.25 mg/ml trypsin/0.01% ethylenediamine tetraacetic acid and subcultured. Second- to fourth-passage NHEKs were used in all the experiments.

NHEKs (10<sup>5</sup>) were seeded in 24-well culture plates, allowed to attach for 24 h, and then incubated with or without FICZ, Glyteer, DMSO, and/or IL-4. Various concentrations of FICZ (10–100 nM), Glyteer (0.0001–0.001%), DMSO, and IL-4 (10 ng/ml) were prepared in the cell culture medium.

**Transfection of siRNAs against AHR and OVOL1.** siRNAs against AHR (AHR siRNA, s1200) or OVOL1 (OVOL1 siRNA, s9393) as well as siRNA consisting of a scrambled sequence that would not lead to specific degradation of any cellular mRNA (control siRNA) were purchased from Ambion (Austin, TX, USA). NHEKs cultured in 24-well plates were incubated for 48 h in 0.5 ml of the culture medium with a mixture containing 5 nM siRNA and 3 μl of the HiPerFect Transfection reagent (Qiagen, Courtabouef, France).

**Plasmid DNA and transfection of plasmids.** Plasmids pCMV6-Entry (Mock) and OVOL1 (Myc-DDK-tagged)-Human ovo-like 1 (*Drosophila*) (OVOL1), which contains a cytomegalovirus promoter and OVOL1 (NM\_004561) human cDNA open reading frame clone, were obtained from Origene (Rockville, MD, USA). The plasmids were transfected into NHEKs using 4D-Nucleofector (Lonza, Basel, Switzerland).

**Quantitative reverse transcription-PCR analysis.** Total RNA was extracted using the RNeasy Mini kit (Qiagen). Reverse transcription was performed using PrimeScript RT reagent kit (Takara Bio, Otsu, Japan). Quantitative reverse transcription (qRT)-PCR was conducted on a CFX Connect Real-time System (Bio-Rad, Hercules, CA, USA) using SYBR Premix Ex Taq (Takara Bio). Amplification was initiated at 95 °C for 30 s as the first step, followed by 40 cycles of qRT-PCR at 95 °C for 5 s and at 60 °C for 20 s. mRNA expression was measured in triplicate and mRNA levels normalized to β-actin were expressed as fold induction relative to the control group. The sequences of primers from Takara Bio are presented in the Supplementary Figure S6.

**Immunofluorescent staining and confocal laser scanning microscopy.** NHEKs (2 × 10<sup>4</sup>) cultured on slides (Lab-Tek, Rochester, NY, USA) with or without IL-4, FICZ, and/or Glyteer were washed in phosphate-buffered saline (PBS), fixed with acetone for 10 min, and blocked using 10% bovine serum albumin in PBS for 30 min. The samples were incubated with an anti-FLG antibody or anti-OVOL1 antibody in WesternBreeze Blocker/Diluent (Invitrogen, Carlsbad, CA, USA)

overnight at 4 °C. The slides were washed with PBS before incubation for 1 h at room temperature with a secondary antibody: an anti-rabbit IgG or anti-mouse IgG antibody (conjugated with Alexa Fluor 488 or Alexa Fluor 546; Molecular Probes, Eugene, OR, USA). After nuclear staining with DAPI, which emits blue fluorescence, slides were mounted with the UltraCruz Mounting Medium (Santa Cruz Biotechnology). The nuclear translocation of OVOL1 in NHEKs was evaluated by detection of the coincidence of the two-color fluorescence (green and blue) in the nucleus. All the samples were analyzed using a D-Eclipse confocal laser scanning microscope (Nikon, Tokyo, Japan).

**IHC analysis of normal skin and AD skin.** This experiment was conducted in accordance with the principles embodied in the Declaration of Helsinki, and was approved by the institutional Ethics Committee.

Ten AD skin samples from 10 AD patients and 10 normal skin samples were used. All the samples were obtained from the archives of the Department of Dermatology of Kyushu University Hospital, Japan. Clinical and demographic data retrieved from the patient files were consistent with a diagnosis of AD.

All samples were fixed with 10% buffered formalin. The archival paraffin-embedded tissue blocks were cut into 4-μm-thick tissue slices. The slices were deparaffinized with xylene for 10 min and rehydrated by means of a graded ethanol series. Antigen retrieval was performed using the Heat Processor Solution pH 6 (Nichirei Biosciences Inc., Tokyo, Japan) at 100 °C for 40 min. The slices were then incubated with an anti-FLG antibody at room temperature for 1 h or an anti-OVOL1 antibody at 4 °C overnight, followed by incubation with a secondary antibody, N-Histofine Simple Stain AP (Nichirei Biosciences Inc.). Immunodetection was conducted with Fast Red (Nichirei Biosciences Inc.), followed by light counterstaining with hematoxylin. The slices stained without a primary antibody served as a negative control.

For semiquantitative analysis of IHC staining, microscopic visual fields of the samples from each group were randomly chosen and examined. In a high-power field (×400 magnification), the nuclear-OVOL1-stained cells of the epidermis were counted, as was the total number of cells with hematoxylin staining.

**3D-cultured NHEKs as human skin equivalents.** The human epidermal 3D model (EpiDem EPI-200; MatTek, Ashland, MA, USA) was incubated with or without Glyteer (0.01%), FICZ (1 μM), and/or CH-223191 (10 μM) for 48 h at 37 °C.

**Western blotting.** Cells were incubated for 5 min in lysis buffer (Complete lysis M; Roche Diagnostics, Basel, Switzerland). The protein concentration in the lysate was measured using a BCA Protein Assay Kit (Thermo Fisher Scientific, Rockford, IL, USA). Equal amounts of protein (20 μg) were dissolved in NuPAGE LDS sample buffer (Invitrogen) and a 10% sample reducing agent (Invitrogen). The lysates were boiled at 70 °C for 10 min and then loaded into and subjected to electrophoresis in NuPAGE 4–12% Bis-Tris gels (Invitrogen) at 200 V for 60 min. The proteins were then transferred onto polyvinylidene difluoride membranes (Invitrogen), and the membranes were blocked with WesternBreeze Blocker/Diluent (Invitrogen). The membranes were then probed with the anti-FLG antibody, anti-OVOL1 antibody, and a mouse monoclonal antibody against human β-actin (anti-β-actin) (Cell Signaling Technology, Danvers, MA, USA) overnight at 4 °C. Horseradish peroxidase-conjugated anti-mouse IgG antibodies (Cell Signaling Technology) served as a secondary antibody. The visualization of protein bands was accomplished with the SuperSignal West Pico Chemiluminescent Substrate (Thermo Scientific) by ChemiDoc touch imaging system (Bio-Rad).

**Cellular nuclear protein preparation for western blot analysis.** NHEKs were treated with FICZ (100 nM) or Glyteer (0.001%) in the absence or presence of IL-4 (10 ng/ml) for 18 h. Cell nuclear protein was collected using NE-PER Nuclear and Cytoplasmic Extraction Reagents (Thermo Fisher Scientific, Rockford, IL, USA). The nuclear OVOL1 expression in NHEKs was analyzed by western blotting. Histone deacetylase 1 (HDAC1) served as an internal loading control. An anti-human HDCA1 antibody was purchased from Cell Signaling Technology.

**Statistical analysis.** Unpaired Student's *t*-test or one-way analysis of variance was used to assess the results. A *P*-value of <0.05 was assumed to indicate a statistically significant difference. All data are presented as mean ± standard error of the mean (S.E.M.) from three independent experiments.

## Conflict of Interest

The authors declare no conflict of interest.

**Acknowledgements.** This work was partly supported by grants from the Ministry of Health, Labour and Welfare, the Research on Development of New Drugs from Japan Agency for Medical Research and Development (AMED), and the Leading Advanced Projects for Medical Innovation (LEAP).

**Author contributions**

GT, AH-H, MK-O, FO, TI, SM-K, CH, TN, MF, and HU designed the experiments and interpreted the results. GT, AH-H, and MT conducted the experiments. The manuscript was written by GT, AH-H, and MF.

1. Kypriotou M, Huber M, Hohl D. The human epidermal differentiation complex: cornified envelope precursors, S100 proteins and the 'fused genes' family. *Exp Dermatol* 2012; **21**: 643–649.
2. Asai Y, Greenwood C, Hull PR, Alizadehfar R, Ben-Shoshan M, Brown SJ *et al*. Filaggrin gene mutation associations with peanut allergy persist despite variations in peanut allergy diagnostic criteria or asthma status. *J Allergy Clin Immunol* 2013; **132**: 239–242.
3. Elias PM, Wakefield JS. Mechanisms of abnormal lamellar body secretion and the dysfunctional skin barrier in patients with atopic dermatitis. *J Allergy Clin Immunol* 2014; **134**: 781–791.
4. Palmer CN, Irvine AD, Terron-Kwiatkowski A, Zhao Y, Liao H, Lee SP *et al*. Common loss-of-function variants of the epidermal barrier protein filaggrin are a major predisposing factor for atopic dermatitis. *Nat Genet* 2006; **38**: 441–446.
5. Park J, Jekarl DW, Kim Y, Kim J, Kim M, Park YM. Novel FLG null mutations in Korean patients with atopic dermatitis and comparison of the mutational spectra in Asian populations. *J Dermatol* 2015; **42**: 867–873.
6. Furue M, Tsuji G, Mitoma C, Nakahara T, Chiba T, Morino-Koga S *et al*. Gene regulation of filaggrin and other skin barrier proteins via aryl hydrocarbon receptor. *J Dermatol Sci* 2015; **80**: 83–88.
7. Takei K, Mitoma C, Hashimoto-Hachiya A, Uchi H, Takahara M, Tsuji G *et al*. Antioxidant soybean tar Glyteer rescues T-helper-mediated downregulation of filaggrin expression via aryl hydrocarbon receptor. *J Dermatol* 2015; **42**: 171–180.
8. Esparza-Gordillo J, Weidinger S, Fölster-Holst R, Bauerfeind A, Ruschendorf F, Patone G *et al*. A common variant on chromosome 11q13 is associated with atopic dermatitis. *Nat Genet* 2009; **41**: 596–601.
9. Sun LD, Xiao FL, Li Y, Zhou WM, Tang HY, Tang XF *et al*. Genome-wide association study identifies two new susceptibility loci for atopic dermatitis in the Chinese Han population. *Nat Genet* 2011; **43**: 690–694.
10. Hirota T, Takahashi A, Kubo M, Tsunoda T, Tomita K, Sakashita M *et al*. Genome-wide association study identifies eight new susceptibility loci for atopic dermatitis in the Japanese population. *Nat Genet* 2012; **44**: 1222–1226.
11. Paternoster L, Standl M, Chen CM, Ramasamy A, Bønnelykke K, Duijts L *et al*. Meta-analysis of genome-wide association studies identifies three new risk loci for atopic dermatitis. *Nat Genet* 2012; **44**: 187–192.
12. Ellinghaus D, Baurecht H, Esparza-Gordillo J, Rodríguez E, Matanovic A, Marenholz I *et al*. High density genotyping study identifies four new susceptibility loci for atopic dermatitis. *Nat Genet* 2013; **45**: 808–812.
13. Tamari M, Hirota T. Genome-wide association studies of atopic dermatitis. *J Dermatol* 2014; **41**: 213–220.

14. Dai X, Schonbaum C, Degenstein L, Bai W, Mahowald A, Fuchs E. The ovo gene required for cuticle formation and oogenesis in flies is involved in hair formation and spermatogenesis in mice. *Genes Dev* 1998; **12**: 3452–3463.
15. Johnson AD, Fitzsimmons D, Hagman J, Chamberlin HM. EGL-38 pax regulates the ovo-related gene lin-48 during *Caenorhabditis elegans* organ development. *Development* 2001; **128**: 2857–2865.
16. Nair M, Teng A, Bilanchone V, Agrawal A, Li B, Dai X. OVOL1 regulates the growth arrest of embryonic epidermal progenitor cells and represses c-myc transcription. *J Cell Biol* 2006; **173**: 253–264.
17. Mitoma C, Nakahara T, Uchi H, Ito T, Inatomi Y, Ide T *et al*. Preferential expression of OVOL1 in inner root sheath of hair, sebaceous gland, eccrine duct and their neoplasms in human skin. *Fukuoka Igaku Zasshi* 2014; **105**: 166–173.
18. Ito T, Tsuji G, Ohno F, Uchi H, Nakahara T, Hashimoto-Hachiya A *et al*. Activation of the OVOL1-OVOL2 axis in the hair bulb and in pilomatricoma. *Am J Pathol* 2016; **186**: 1036–1043.
19. Kwa MQ, Huynh J, Aw J, Zhang L, Nguyen T, Reynolds EC *et al*. Receptor-interacting protein kinase 4 and interferon regulatory factor 6 function as a signaling axis to regulate keratinocyte differentiation. *J Biol Chem* 2014; **289**: 31077–31087.
20. Tsuji G, Takahara M, Uchi H, Matsuda T, Chiba T, Takeuchi S *et al*. Identification of ketoconazole as an AhR-Nrf2 activator in cultured human keratinocytes: the basis of its anti-inflammatory effect. *J Invest Dermatol* 2012; **132**: 59–68.
21. Van den Bogaard EH, Bergboer JG, Vonk-Bergers M, van Vlijmen-Willems IM, Hato SV, van der Valk PG *et al*. Coal tar induces AHR-dependent skin barrier repair in atopic dermatitis. *J Clin Invest* 2013; **123**: 917–927.
22. Howell MD, Kim BE, Gao P, Grant AV, Boguniewicz M, De Benedetto A *et al*. Cytokine modulation of atopic dermatitis filaggrin skin expression. *J Allergy Clin Immunol* 2007; **120**: 150–155.
23. Lee B, Villarreal-Ponce A, Fallahi M, Ovadia J, Sun P, Yu QC *et al*. Transcriptional mechanisms link epithelial plasticity to adhesion and differentiation of epidermal progenitor cells. *Dev Cell* 2014; **29**: 47–58.
24. Kang Z, Li Q, Fu P, Yan S, Guan M, Xu J *et al*. Correlation of KIF3A and OVOL1, but not ACTL9, with atopic dermatitis in Chinese pediatric patients. *Gene* 2015; **571**: 249–251.
25. Wei YD, Rannug U, Rannug A. UV-induced CYP1A1 gene expression in human cells is mediated by tryptophan. *Chem Biol Interact* 1999; **118**: 127–140.



**Cell Death and Disease** is an open-access journal published by **Nature Publishing Group**. This work is licensed under a **Creative Commons Attribution 4.0 International License**. The images or other third party material in this article are included in the article's Creative Commons license, unless indicated otherwise in the credit line; if the material is not included under the Creative Commons license, users will need to obtain permission from the license holder to reproduce the material. To view a copy of this license, visit <http://creativecommons.org/licenses/by/4.0/>

© The Author(s) 2017

Supplementary Information accompanies this paper on Cell Death and Disease website (<http://www.nature.com/cddis>)